



ELSEVIER

Contents lists available at ScienceDirect

Opto-Electronics Review

journal homepage: <http://www.journals.elsevier.com/opto-electronics-review>

Magneto spectroscopy of double HgTe/CdHgTe QWs with inverted band structure in high magnetic fields up to 30 T

L.S. Bovkun^{a,b}, A.V. Ikonnikov^{a,c,*}, V.Ya. Aleshkin^{a,d}, K.V. Maremyanin^{a,d},
N.N. Mikhailov^e, S.A. Dvoretiskii^e, S.S. Krishtopenko^{a,f}, F. Teppe^f, B.A. Piot^b,
M. Potemski^b, M. Orlita^{b,g}, V.I. Gavrilenko^{a,d}

^a Institute for Physics of Microstructures – Branch of Federal Research Center “Institute of Applied Physics of Russian Academy of Sciences”, 603950 Nizhny Novgorod, Russia

^b Laboratoire National des Champs Magnétiques Intenses, LNCMI - CNRS - UGA - UPS - INSA - EMFL, 38042 Grenoble, France

^c Faculty of Physics, M.V. Lomonosov Moscow State University, 119991 Moscow, Russia

^d Lobachevsky State University of Nizhny Novgorod, 603950 Nizhny Novgorod, Russia

^e Institute of Semiconductor Physics, Siberian Branch RAS, 630090 Novosibirsk, Russia

^f Laboratoire Charles Coulomb (L2C), UMR CNRS 5221, GIS - TERALAB, Université Montpellier II, F34095 Montpellier, France

^g Institute of Physics, Charles University, 12116 Prague, Czech Republic

ARTICLE INFO

Article history:

Received 21 December 2018

Received in revised form 16 April 2019

Accepted 2 June 2019

Keywords:

HgTe/CdHgTe heterostructures

Double quantum wells

Far-IR magneto spectroscopy

Landau levels

ABSTRACT

Magnetoabsorption in far and mid IR ranges in double HgTe/CdHgTe quantum wells with inverted band structure has been studied in high magnetic fields up to 30 T. Numerous intraband and interband transitions have been revealed in the spectra and interpreted within axial 8×8 k·p model. Splitting of dominant magnetoabsorption lines resulting from optical transitions from hole-like zero-mode Landau level has been discovered and discussed in terms of a built-in electric field and collective phenomena.

© 2019 Association of Polish Electrical Engineers (SEP). Published by Elsevier B.V. All rights reserved.

Introduction

HgTe quantum wells (QWs) possess remarkable physical properties. One of the most important features of the HgTe QWs is the possibility of band inversion. The barrier material ($\text{Cd}_{0.7}\text{Hg}_{0.3}\text{Te}$ in our case) has a normal band ordering, with the *s*-type Γ_6 band lying above the *p*-type Γ_8 band as in ordinary semiconductor, while in the HgTe the Γ_6 band lies below the Γ_8 band, corresponding to an inverted band ordering [1]. In HgTe QW, depending on its width *d*, various band ordering can also be realized. If the QW width *d* is less than critical value $d_c \approx 6.3$ nm, the lowest subband in the conduction band E1 is formed by $|\Gamma_6, \pm 1/2\rangle$ states and light-hole $|\Gamma_8, \pm 1/2\rangle$ states, while the first valence subband H1 arises from the $|\Gamma_8, \pm 3/2\rangle$ states, corresponding to the heavy-hole band. This is called the normal band structure, since the electron-like subband E1 lies above the hole-like subband H1, and this corresponds to the trivial insulator phase. When the QW width *d* exceeds the critical width d_c

the inversion occurs and the electron-like subband E1 lies below the hole-like subband H1 and this arrangement gives rise to spin-polarized helical edge states and topological insulator (TI) phase [2,3].

The inverted band ordering also causes an unconventional behaviour of Landau levels (LLs). The lowest LL in the conduction band has a hole-like character and tends toward low energies with increasing magnetic field. At the same time, one of the valence band's LL has electron-like character and increases in energy with the magnetic field. These levels are so-called “zero-mode” LLs. At certain magnetic field B_c zero-mode LLs cross (or avoid crossing) each other [3–9].

At $d = d_c$ the band structure of the HgTe QW is gapless and the system becomes a “single-valley” analog of graphene [10].

Recently, a new two-dimensional (2D) system, double HgTe quantum wells (DQW) with a tunnel-transparent CdHgTe barrier was proposed [11] that could demonstrate more fascinating and still unrevealed features. In this system, in addition to the trivial insulator, gapless state with massless Dirac fermions and TI phases, new phases can be realized. For example, a specific metal phase, in which a gapless bulk and a pair of helical edge states coexist, can be formed in a wide range of QW and barrier layer thicknesses.

* Corresponding author at: Faculty of Physics, M.V. Lomonosov Moscow State University, 119991 Moscow, Russia.

E-mail address: antikonn@physics.msu.ru (A.V. Ikonnikov).

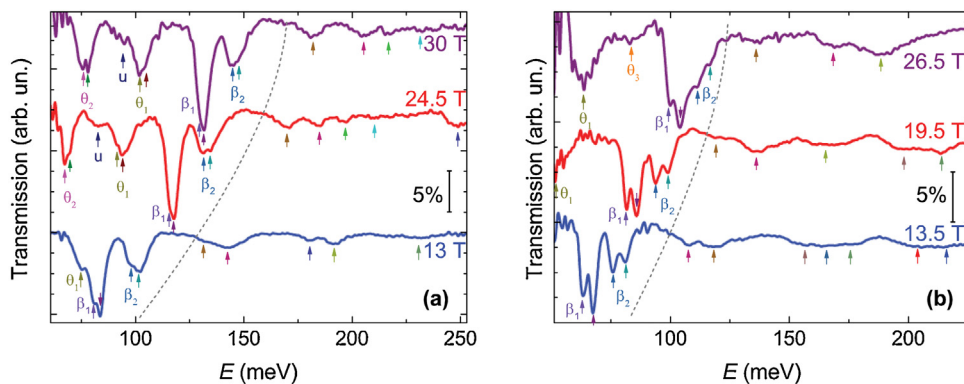


Fig. 1. Typical magnetoabsorption spectra in samples A (a) and B (b), measured in different magnetic fields. The arrows indicate the observed spectral features. The dotted line denotes the symbolic boundary between low-frequency and high-frequency lines.

Table 1

Growth and real (in brackets) parameters and 2D hole concentrations of the samples under study.

Sample	d_{QW} , nm	t_{bar} , nm	x	p_s , 10^{11} cm $^{-2}$
A (150218)	6.5 (6.3)	3.0 (2.8)	0.71	0.7
B (150219)	8.4 (8.4)	3.0 (2.8)	0.67	1.7

This phase holds some properties of a bilayer graphene such as an unconventional quantum Hall effect and an electrically-tunable band gap [11]. Moreover, in DQW with wider wells the inversion between second electron- and hole-like subbands takes place that leads to the doubling of zero-mode LL (anti)crossing.

To date, HgTe DQW band structure investigations by magneto-optical spectroscopy have been performed in a structure with normal band ordering [12] and in that in “bilayer graphene” phase (sample A) in magnetic fields up to 12 T [12–14] only. A “doubling” of the main absorption lines resulting from the separating barrier transparency for the electron-like states was demonstrated. In Ref. 13 spectra of Faraday rotation were measured for the first time thus enabling to determine the sign of circular polarization and unambiguous interpretation of observed magneto-optical transitions. Also, in Refs. 15 and 16 HgTe DQW in “bilayer graphene” phase (sample A in our work) an unusual reentrant Quantum Hall Effect was discovered and attributed to the peculiarities of a complicated LL structure in the valence band. In this work magneto-optical studies are extended to higher magnetic fields up to 30 T where strong magnetic quantization overcomes effects of state mixing due to bulk and interface inversion asymmetry (cf. [8]). The latter allows to identify unambiguously all spectral features and to reveal the splitting of zero-mode Landau levels.

Experimental

The samples under study were grown by molecular beam epitaxy (MBE) on semi-insulating GaAs (013) substrates with ellipsometric control of the layer composition and thickness [17]. To eliminate large lattice mismatch of HgCdTe heterostructure and GaAs substrate a thick (5 μm) relaxed CdTe buffer was grown. The active part of the structure consisted of a 30-nm lower Hg $_{1-x}$ Cd $_x$ Te barrier, two HgTe QWs of width d_{QW} separated by a tunnel-transparent Hg $_{1-x}$ Cd $_x$ Te barrier of thickness t_{bar} , and a 30-nm upper Hg $_{1-x}$ Cd $_x$ Te barrier. At last, 40-nm-thick CdTe cap layer was grown. The structures were not intentionally doped; as-grown samples were of p -type due to native defects (mercury vacancies). The parameters of the structures are presented in Table 1. Typical mobility values at low temperatures were about 5×10^4 cm 2 /V.s.

Magnetoabsorption spectra were measured in the Laboratoire National des Champs Magnétiques Intenses in Grenoble (France)

using Fourier-transform spectrometer Bruker Vertex 80v. We used Globar as a radiation source and composite silicon bolometer as a detector. The radiation from spectrometer was guided through suitable entrance window of the sealed probe, delivered via light-pipe optics to the sample and detector placed below the sample. All measurements were made in Faraday geometry. The spectral resolution was 8 cm $^{-1}$. Typical sample dimensions were 5 \times 5 mm. We used two types of magnets for generating magnetic field: superconducting solenoid for fields up to 11 T and resistive solenoid for fields up to 30 T. Black polyethylene, white polyethylene, ZnSe or Ge windows were used in the measurements with 11 T superconducting solenoid depending on the spectral range explored. In experiments with 30 T resistive solenoid we used Ge window only which is opaque below 49 meV. In experiments with 11 T solenoid we were able to change the carrier concentration by blue LED illumination (taking advantage of the persistent photoconductivity effect, see, e.g., [8,18,19]). In what follows we present the magnetoabsorption data obtained in both type experiments with the same hole concentration given in Table 1. The measured transmission spectra were normalized to the transmission spectrum in zero magnetic field and to the transmission of the reference channel without sample. The last action allowed us to correct the field-induced changes in the response of the bolometer. Experiments with superconducting solenoid were performed at $T=4.2$ K, experiments with resistive solenoid were performed at $T=1.6$ K.

Results and discussion

Fig. 1 shows typical magnetoabsorption spectra measured in the samples A and B. We fit each spectrum with multiple Lorentzians and determined the position, the width, and the area of each spectral feature. To identify the magnetoabsorption lines we calculate LL energies, wave functions, and probabilities of optical transitions between LL for the unpolarized radiation. LL spectra were calculated by the diagonalization the 8×8 k-p Hamiltonian for (013)-oriented heterostructures [6,18] with material parameters from Ref. 20. A tensile strain in individual layers arising due to the mismatch of lattice constants in the CdTe buffer, HgTe QW, and Cd $_x$ Hg $_{1-x}$ Te barriers was also taken into account. In addition, an electric field parallel to the structure growth axis was taken into account to explain the observed splitting of dominant magnetoabsorption lines (β_1 and β_2). This electric field is built-in; it is responsible, for example, for the effect of residual photoconductivity [19]. We used the axial approximation for the Hamiltonian [6,8,11], thus also neglecting Bulk Inversion Asymmetry (BIA) and Interface Inversion Asymmetry (IIA) terms, since their influence decreases with the magnetic field [8]. To achieve the best agreement between calculations and experimental data we slightly

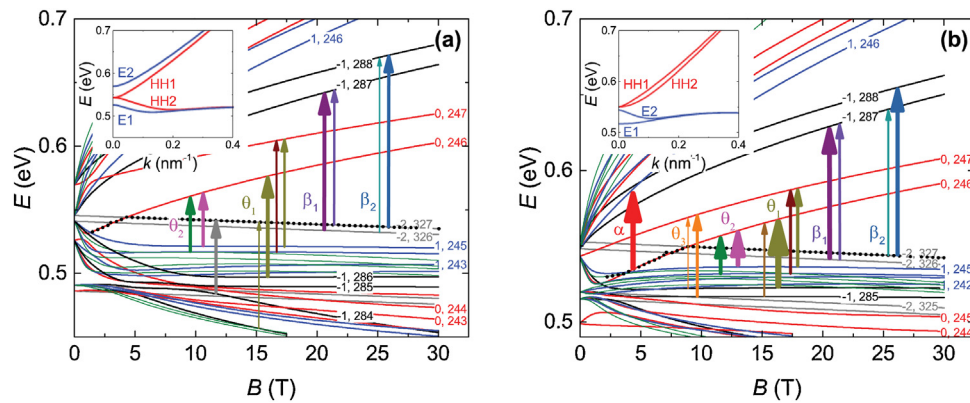


Fig. 2. Calculated LLs taking into account the built-in vertical electric field $E = 5$ kV/cm in the sample A (a) and $E = 4$ kV/cm in the sample B (b). The arrows indicate several dominant magneto-optical transitions. The thickness of the arrows represent the characteristic transition probabilities/ Broken dotted lines are the position of the Fermi levels for the hole concentration $0.7 \cdot 10^{11} \text{ cm}^{-2}$ (a) and $1.7 \cdot 10^{11} \text{ cm}^{-2}$ (b). The insets show calculated energy-momentum laws ($E = 0, B = 0, \mathbf{k} \parallel [100]$).

adjusted the parameters of our structures (see Table 1). Both structures were grown one by one, and real (adjusted) parameters d_{QW} and t_{bar} are slightly less than the growth ones for both structures. Calculated LLs are given in Fig. 2. Each level is characterized by the LL index n ($n = -2, -1, 0, 1, \dots$). The second number is an “internal” number used in our calculations. A pair of these numbers uniquely identifies a specific LL. Energy-momentum laws in the absence of magnetic field are given in the insets on Fig. 2(a) and Fig. (b). As easy to see the band structure of the sample A is inverted and corresponds to the “bilayer graphene phase: the top of the valence band and the bottom of the conduction band are formed by heavy hole (HH) states (“parabolic” HH1 and HH2 subbands touching at $k=0$ since the separating barrier is opaque for heavy holes). LLs $n = -2$ are split because of built-in electric field. The upper hole-like LLs $n = -2$ “belongs” to the conduction band up to the crossing at $B \approx 4.2$ T with the electron-like LL $n = 0$ originating from the second electron-like valence subband E2. The band structure of the sample B is “double inverted”: two lowest subbands in the conduction band are hole-like (HH1 and HH2) while to top subbands in the valence band (E2 and E1) are electron-like. Correspondingly, two electron-like LLs $n = 0, 246 \& 247$ originating from E2 and E1 subbands increases in energy with the magnetic field and cross hole-like LLs $n = -2, 326 \& 327$ originating from HH2 and HH1 subbands.

Experimental and calculation results are summarized in Fig. 3 and Fig. 4. Each symbol corresponds to a certain peak in the magnetoabsorption spectra. The symbol area is proportional to the integral intensity of a peak; the error bar represents the peak’s full width at half maximum. One can see that the results of the measurements in moderate magnetic fields up to 11 T and in high magnetic fields up to 30 T coincide fairly well. Some discrepancies are most likely results from a slight difference between the samples cut from the same wafers used in the measurements with superconductive and resistive solenoids.

In Fig. 3, one can distinguish two main areas of magneto-optical transitions: “low-frequency” (up to β_2) and “high-frequency” ones, separated by a gap at 100–150 meV (cf. [8]). In the sample A the LL filling factor ν is less than unity for the magnetic fields above 2.9 T, i.e. in higher fields Fermi level is at the upper hole Landau level. In what follows we’ll mainly discuss optical transitions in magnetic fields over 11 T, since in lower fields they have been identified Refs. 12 and 13. At $B > 4.2$ T (crossing of the upper $n = -2$ and $n = 0$ LLs) the Fermi level is at $n = -2, 327$ LL Fig. 2(a)] that is partially filled with electrons. Therefore, in these fields we can observe either interband transitions, or intraband transitions involving only the above-mentioned $n = -2, 327$ LL.

Let us start from the consideration of the high-frequency lines which all results from interband transitions. One can see in Fig. 3

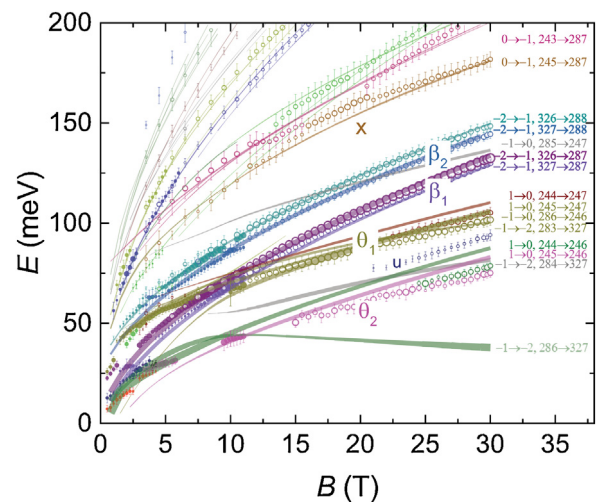


Fig. 3. Positions of observed magnetoabsorption lines versus the magnetic field in the sample A (open symbols correspond to the measurements in the magnetic fields up to 30 T, solid symbols correspond to the measurements in fields up to 11 T) and calculated energies of possible transitions (curves). Error bars show the features’ full width at half maximum. The area of a symbol is proportional to an integral intensity of the magnetoabsorption line; the thickness of the curves is proportional to the transitions’ probabilities (taking into account LL degeneracy).

the general trade of an absorption line intensity decreases with the energy that reflects the inverse proportionally of the transition probability on the frequency (see, e.g., [8]). We calculated energies and the probabilities of the optical transitions between LL with the same spin orientation, which satisfied the selection rules for electric-dipole excitations $\Delta n = \pm 1$. In Fig. 3 we plot all the transitions with a significant probability, actually they involve LLs with $n \leq 2$. One can see that for almost all allowed transitions the corresponding lines are observed. Some lines correspond to multiple transitions and split in high magnetic fields (for example, X line, Fig. 3). We traced the high-frequency lines up to 300 meV and found a good agreement between the lines’ positions and calculated transitions. We do not present all the data in Fig. 3 and Fig. 4 to avoid cluttering.

The low-frequency magnetoabsorption in high magnetic fields is represented by 5 lines: $\beta_1, \beta_2, \theta_1, \theta_2$ and u (Fig. 3). The lines β_1 and β_2 correspond to a well known $-2 \rightarrow -1$ transitions from one of the zero-mode LL $n = -2$ to LL $n = -1$ in the conduction band [4–7]. In a DQW system, the presence of a tunnel-transparent barrier leads to interaction of states in different QWs resulting in doubling of electron-like $n = -1$ LL [12,13]. That is why we have two $-2 \rightarrow -1$

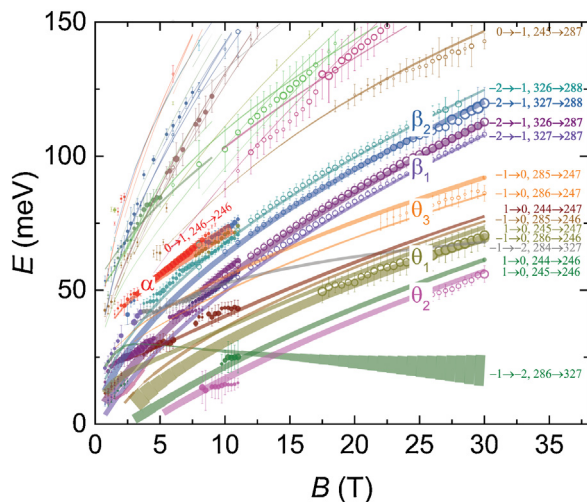


Fig. 4. Positions of observed magnetoabsorption lines versus the magnetic field in the sample A (open symbols correspond to the measurements in the magnetic fields up to 30 T, solid symbols correspond to the measurements in fields up to 11 T) and calculated energies of possible transitions (curves). Error bars show the features' full width at half maximum. The area of a symbol is proportional to an integral intensity of the magnetoabsorption line; the thickness of the curves is proportional to the transitions' probabilities (taking into account LL degeneracy).

transitions (β_1 and β_2 lines) instead of the one in a single HgTe QW. Lines θ_1 and θ_2 seem to consist of multiple transitions. They were earlier observed in Refs. 12 and 13, but their interpretation was not unambiguous. In recent work [13] Faraday rotation measurements showed that in magnetic fields over 6 T θ_1 line resulted from transitions with $\Delta n = +1$ while and θ_2 line to those with $\Delta n = -1$. Measurements in high magnetic fields allowed revealing splitting both θ_1 and θ_2 lines [Fig. 1(a) and Fig. 3]. One can see in Fig. 3 that there are four allowed transitions with energies closed to θ_1 line and the most strong one $-1 \rightarrow 0$ (286 \rightarrow 246) indeed correspond to the condition $\Delta n = +1$. As for θ_2 line, there are two strong enough transitions $1 \rightarrow 0$ (244 \rightarrow 246) and $1 \rightarrow 0$ (245 \rightarrow 246) both satisfying the condition $\Delta n = -1$ (Fig. 3). The origin of a weak u line, that arise in the spectra in magnetic fields over 20 T, is not quite clear, probably it results from a transition that we attributed to θ_1 or θ_2 lines. At last, the predicted low frequency $-1 \rightarrow -2$ (286 \rightarrow 327) transition (Fig. 3) arising in high magnetic field does not appear in spectra since its energy is quite below the low-frequency cut-off of 50 meV of Ge window used in 30 T experiment.

A similar magnetoabsorption picture is observed the in sample B (Fig. 4): high-frequency and low-frequency lines can also be distinguished. High-frequency lines, in the vast majority of cases, are caused by several interband transitions. In the “low-frequency” region of lines, all the dominant magnetoabsorption lines observed

as the sample A ($\beta_1, \beta_2, \theta_1, \theta_2$) are present as well but their energies are significantly lower. The latter is a sequence of a general trade of an increase of electron “effective masses” with QW width in the case of inverted band ordering (in contrast to normal one) firstly demonstrated for single HgTe/CdHgTe QWs [18]. A new absorption line θ_3 seems to result from transitions $-1 \rightarrow 0$ (285 \rightarrow 247) and $-1 \rightarrow 0$ (286 \rightarrow 247). It was not recognized in absorption spectra of the sample A probably because of a superposition with strong β_1 and β_2 lines.

The strong line α observed in fields up to 10 T (Fig. 4) is well-known transition $0 \rightarrow 1$ [4–7]. In our case, it is a transition between LLs 0, 246 and 1, 246 (Fig. 2). The vanishing of the line α is due to the depopulation of LL $n = 0, 246$, when it (anti)crosses the level of $n = -2, 327$.

The peculiarities of the absorption in magnetic fields around 2–3 T and 8–9 T corresponding to (anti)crossing of $n = 0$ LLs with $n = -2$ ones will be discussed elsewhere. Thus, a good agreement between the experimental data and the calculated transition energies for both samples allows us to claim the applicability of the axial approximation in strong magnetic fields in HgTe DQWs.

Let us now proceed to the most intriguing part of the work. One can see that β_1 and β_2 lines ($-2 \rightarrow -1$ transitions) are split (Fig. 1, Fig. 3 and Fig. 4) that intuitively implies splitting of zero-mode $n = -2$ LL. Such splitting should arise if DQW is not symmetrical. Experiments in the set up with superconducting solenoid where it is possible to change the carrier concentration due to the persistent photoconductivity effect have shown that the splitting depends on the hole concentration. So, it seems that DQW asymmetry is likely to result from a built-in electric field (that is tuned by changing hole concentration [19]) rather than from a difference in QW widths. In particular, for the sample B, in order to obtain the observed splitting of 4.5 meV (Fig. 5), the difference in QW width should be 2 nm, that exceeds the “technological accuracy” (± 0.3 nm) several times. Also we calculated LLs taking into account BIA & IIA [7,8] and found that these effects do not lead to any significant splitting of these -2 levels in the DQW: the splitting increases with the field up to 1 meV at 30 T only. Therefore, we excluded the BIA and IIA from the consideration.

The experimental data on β_1 and β_2 lines splitting versus the magnetic field are summarized in Fig. 5. The results are given for magnetic fields over 10 T since in less fields they are highly scattered because of superposition of various optical transitions resulted from LL mixing (BIA and IIA effects). One can see that the splitting seems to be nearly independent on the magnetic field within the experimental accuracy. The average values of the splitting are about 3.5 meV for the sample A and 4.5 meV for the sample B. To obtain such values of $n = -2$ LL splitting we assumed the built-in electric field to be of 5 kV/cm for the sample A and 4 kV/cm for the sample B, see Fig. 2 (that is much less than $4\pi e p_s$ in both cases,

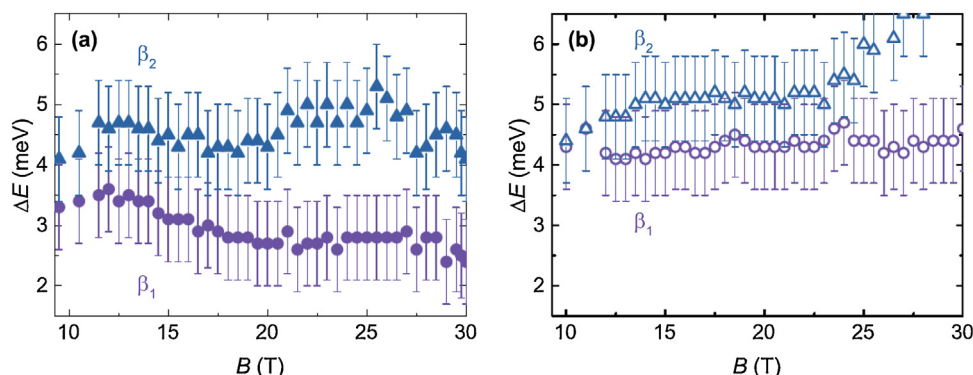


Fig. 5. The values of splitting of β_1 and β_2 lines in the samples A (a) and B (b) versus the magnetic field. Errors are estimated as the square root of twice the spectral resolution.

where e is elementary charge). Thus, the presence of the built-in electric field that is obviously tuned by changing the hole concentration due to persistent photoconductivity effect (recharging the remote carrier traps, cf. [19]) could explain, at least qualitatively, the observed splitting of the dominant β_1 and β_2 magnetoabsorption lines. It is worth noting that such splitting opening the gap in the energy spectrum in HgTe/CdHgTe QW in “bilayer graphene” phase at the external electric field was discussed in Ref. 11 and considered as a power tool to provide electrical switching between semimetal and isolator phase with large gap in contrast to the single QW.

However, as easy to see from Fig. 5, in both samples β_2 line splitting systematically exceeds that of β_1 one. This fact seems to be incompatible with the above “single particle” picture of $n = -2$ LL splitting. One can speculate on mixing and interaction not the single particle states but optical transitions with close energies just as it was revealed in other 2D systems, say in InAs/AlSb QWs [21,22]. Such interaction/mixing of optical transition is also influenced by the carried concentration that could explain the observed splitting dependence on the hole concentration. Definitely, this issue requires future explorations, both theoretical and experimental.

Conclusions

To conclude, we have experimentally studied a magnetoabsorption in two undoped p -type HgTe/CdHgTe DQWs with inverted band structure in high magnetic fields up to 30 T. In addition to earlier observed doubling of dominant magneto-optical transition, resulting from the transparency of separating barrier for the electron-like states, we have revealed a number of interband transitions. Utilization of high magnetic fields has allowed splitting of magnetoabsorption lines resulting from close in energy transitions between different Landau levels. We have found that the observed features can be fairly well described in the framework of axial 8×8 k-p model, at least in high magnetic fields. We have discovered a sufficient splitting of dominant magnetoabsorption lines resulting from optical transitions from hole-like zero-mode Landau level and showed that it can be explained by the level splitting in a built-in electric field. Finally, we speculate that the noticeable difference in the splitting of two dominant lines resulting from the transitions from the same split-of Landau level indicates the importance of collective phenomena on magneto-optical transitions.

CRedit authorship contribution statement

L.S. Bovkun: Conceptualization, Investigation, Formal analysis.
A.V. Ikonnikov: Conceptualization, Writing - original draft, Formal analysis, Visualization.
V.Ya. Aleshkin: Methodology, Software.
K.V. Maremyanin: Formal analysis, Visualization.
N.N. Mikhailov: Resources.
S.A. Dvoretiskii: Resources.
S.S. Krishtopenko: Methodology, Validation.
F. Teppe: Validation.
B.A. Piot: Investigation.
M. Potemski: Project administration, Funding acquisition.
M. Orlita: Supervision, Writing - review & editing.
V.I. Gavrilenko: Writing - review & editing, Funding acquisition, Project administration.

Acknowledgements

This work was supported by the Russian Science Foundation (Grant # 16-12-10317). The authors acknowledge the support of LNCMI-CNRS, a member of the European Magnetic Field Laboratory (EMFL).

References

- [1] A. Rogalski, HgCdTe infrared detector material: history, status and outlook, Rep. Prog. Phys. 68 (2005) 2267–2336, <http://dx.doi.org/10.1088/0034-4885/68/10/R01>.
- [2] B.A. Bernevig, T.L. Hughes, S.-C. Zhang, Quantum spin hall effect and topological phase transition in HgTe quantum wells, Science 314 (2006) 1757–1761, <http://dx.doi.org/10.1126/science.1133734>.
- [3] M. König, S. Wiedmann, C. Brune, A. Roth, H. Buhmann, L.W. Molenkamp, X.-L. Qi, S.-C. Zhang, Quantum spin hall insulator state in HgTe quantum wells, Science 318 (2007) 766–770, <http://dx.doi.org/10.1126/science.1148047>.
- [4] M. Schultz, U. Merkt, A. Sonntag, U. Rössler, R. Winkler, T. Colín, P. Helgesen, T. Skauli, S. Løvold, Crossing of conduction- and valence-subband Landau levels in an inverted HgTe/CdTe quantum well, Phys. Rev. B 57 (1998) 14772–14775, <http://dx.doi.org/10.1103/PhysRevB.57.14772>.
- [5] M. Orlita, K. Masztalerz, C. Faugeras, M. Potemski, E.G. Novik, C. Brune, H. Buhmann, L.W. Molenkamp, Fine structure of zero-mode Landau levels in HgTe/Hg_xCd_{1-x}Te quantum wells, Phys. Rev. B 83 (2011) 115307, <http://dx.doi.org/10.1103/PhysRevB.83.115307>.
- [6] M. Zholudev, F. Teppe, M. Orlita, C. Consejo, J. Torres, N. Dyakonova, M. Czapkiewicz, J. Wrobel, G. Grabecki, N. Mikhailov, S. Dvoretiskii, A. Ikonnikov, K. Spirin, V. Aleshkin, V. Gavrilenko, W. Knap, Magnetospectroscopy of two-dimensional HgTe-based topological insulators around the critical thickness, Phys. Rev. B 86 (2012) 205420, <http://dx.doi.org/10.1103/PhysRevB.86.205420>.
- [7] M.S. Zholudev, F. Teppe, S.V. Morozov, M. Orlita, C. Consejo, S. Ruffenach, W. Knap, V.I. Gavrilenko, S.A. Dvoretiskii, N.N. Mikhailov, Anticrossing of Landau levels in HgTe/CdHgTe (013) quantum wells with an inverted band structure, JETP Lett. 100 (2015) 790–794, <http://dx.doi.org/10.1134/S0021364014240175>.
- [8] L.S. Bovkun, A.V. Ikonnikov, V.Ya. Aleshkin, K.E. Spirin, V.I. Gavrilenko, N.N. Mikhailov, S.A. Dvoretiskii, F. Teppe, B.A. Piot, M. Potemski, M. Orlita, Landau level spectroscopy of valence bands in HgTe quantum wells: Effects of symmetry lowering, J. Phys. Condens. Matter 31 (2019) 45501, <http://dx.doi.org/10.1088/1361-648X/aafdf0>.
- [9] A.M. Kadykov, S.S. Krishtopenko, B. Jouault, W. Desrat, W. Knap, S. Ruffenach, C. Consejo, J. Torres, S.V. Morozov, N.N. Mikhailov, S.A. Dvoretiskii, F. Teppe, Temperature-induced topological phase transition in hgte quantum wells, Phys. Rev. Lett. 120 (2018) 086401, <http://dx.doi.org/10.1103/PhysRevLett.120.086401>.
- [10] B. Büttner, C.X. Liu, G. Tkachov, E.G. Novik, C. Brüne, H. Buhmann, E.M. Hankiewicz, P. Recher, B. Trauzettel, S.C. Zhang, L.W. Molenkamp, Single valley Dirac fermions in zero-gap HgTe quantum wells, Nat. Phys. 7 (2011) 418–422, <http://dx.doi.org/10.1038/nphys1914>.
- [11] S.S. Krishtopenko, W. Knap, F. Teppe, Phase transitions in two tunnel-coupled HgTe quantum wells: bilayer graphene analogy and beyond, Sci. Rep. 6 (2016) 30755, <http://dx.doi.org/10.1038/srep30755>.
- [12] L.S. Bovkun, S.S. Krishtopenko, A.V. Ikonnikov, V.Ya. Aleshkin, A.M. Kadykov, S. Ruffenach, C. Consejo, F. Teppe, W. Knap, M. Orlita, B. Piot, M. Potemski, N.N. Mikhailov, S.A. Dvoretiskii, V.I. Gavrilenko, Magnetospectroscopy of double HgTe/CdHgTe quantum wells, Semiconductors 50 (2016) 1532–1538, <http://dx.doi.org/10.1134/S1063782616110063>.
- [13] L.S. Bovkun, A.V. Ikonnikov, V.Ya. Aleshkin, S.S. Krishtopenko, N.N. Mikhailov, S.A. Dvoretiskii, M. Potemski, B. Piot, M. Orlita, V.I. Gavrilenko, Polarization-sensitive fourier-transform spectroscopy of HgTe/CdHgTe quantum wells in the far infrared range in a magnetic field, JETP Lett. 108 (2018) 329–334, <http://dx.doi.org/10.1134/S0021364018170058>.
- [14] M. Marcinkiewicz, S.S. Krishtopenko, S. Ruffenach, C. Consejo, D. But, A.M. Kadykov, A.M. Fadeev, S.V. Morozov, N.N. Michailov, S.A. Dvoretiskii, V.I. Gavrilenko, W. Knap, F. Teppe, THz magnetospectroscopy of double HgTe quantum well, IEEE Xplore: 41st International Conference on Infrared, Millimeter, and Terahertz Waves (IRMMW-THz) (2016), <http://dx.doi.org/10.1109/IRMMW-THz.2016.7758790>.
- [15] M.V. Yakunin, S.S. Krishtopenko, S.M. Podgornykh, M.R. Popov, V.N. Neverov, N.N. Mikhailov, S.A. Dvoretiskii, HgTe/CdHgTe double quantum well with a spectrum of bilayer graphene and peculiarities of its magnetotransport, JETP Lett. 104 (2016) 403–410, <http://dx.doi.org/10.1134/S0021364016180132>.
- [16] M.V. Yakunin, S.S. Krishtopenko, S.M. Podgornykh, M.R. Popov, V.N. Neverov, B. Jouault, W. Desrat, F. Teppe, S.A. Dvoretiskii, N.N. Mikhailov, Unconventional Reentrant Quantum Hall Effect in a HgTe/CdHgTe Double Quantum Well, 2018, arXiv:1811.06791v1.
- [17] S. Dvoretiskii, N. Mikhailov, Y. Sidorov, V. Shvets, S. Danilov, B. Wittman, S. Ganichev, Growth of HgTe quantum wells for IR to THz detectors, J. Electron. Mater. 39 (2010) 918–923, <http://dx.doi.org/10.1007/s11664-010-1191-7>.
- [18] A.V. Ikonnikov, M.S. Zholudev, K.E. Spirin, A.A. Lastovkin, K.V. Maremyanin, V.Ya. Aleshkin, V.I. Gavrilenko, O. Drachenko, M. Helm, J. Wenz, M. Goiran, N.N. Mikhailov, S.A. Dvoretiskii, F. Teppe, N. Diakonova, C. Consejo, B. Chenaud, W. Knap, Cyclotron resonance and interband optical transitions in HgTe/CdTe(013) quantum well heterostructures, Semicond. Sci. Technol. 26 (2011) 125011, <http://dx.doi.org/10.1088/0268-1242/26/12/125011>.
- [19] K.E. Spirin, D.M. Gaponova, K.V. Maremyanin, V.V. Rumyantsev, V.I. Gavrilenko, N.N. Mikhailov, S.A. Dvoretiskii, Bipolar persistent photoconductivity effects in HgTe/CdHgTe (013) double quantum well heterostructures, Semiconductors 52 (2018) 1586, <http://dx.doi.org/10.1134/S1063782618120230>.

- [20] E.G. Novik, A. Pfeuffer-Jeschke, T. Jungwirth, V. Latussek, C.R. Becker, G. Landwehr, H. Buhmann, L.W. Molenkamp, Band structure of semimagnetic $\text{Hg}_{1-y}\text{Mn}_y\text{Te}$ quantum wells, *Phys. Rev. B* 72 (2005), 035321, <http://dx.doi.org/10.1103/PhysRevB.72.035321>.
- [21] A. Ikonnikov, S. Krishtopenko, V. Gavrilenko, Yu. Sadofyev, Yu. Vasilyev, M. Orlita, W. Knap, Splitting of cyclotron resonance line in InAs/AlSb QW heterostructures in high magnetic fields: effects of electron-electron and electron-phonon interaction, *J. Low Temp. Phys.* 159 (2010) 197–202, <http://dx.doi.org/10.1007/s10909-009-0151-1>.
- [22] S.S. Krishtopenko, A.V. Ikonnikov, M. Orlita, Yu.G. Sadofyev, M. Goiran, F. Teppe, W. Knap, V.I. Gavrilenko, Effect of electron-electron interaction on cyclotron resonance in high-mobility InAs/AlSb quantum wells, *J. Appl. Phys.* 117 (2015), 112813, <http://dx.doi.org/10.1063/1.4913927>.